

Development of a Real-Time Absorption Method for Detecting the Mercaptan Odorizing Mixture of Natural Gas

S. V. Kireev¹, N. G. Petrov², E. M. Podolyako¹, and S. L. Shnyrev¹

¹ *Moscow Engineering Physics Institute (State University), Kashirskoe sh. 31, Moscow, 115409 Russia*

² *DOAO Orgenergogaz, Luganskaya ul. 11, Moscow, 115304 Russia*

e-mail: kireev@eai.mephi.ru, shnyrev@inbox.ru

Received December 11, 2004

Abstract—The absorption of mercaptan mixtures used for odorizing natural gas and mixtures of natural gas is experimentally studied in the spectral range 2.5–20 μm . An absorption method for the real-time detection of the odorant concentration is proposed. The method is based on intensity measurements of the radiation that has passed through the absorbing medium at three wavelengths corresponding to the absorption maxima of the odorant components. The sensitivity of the odorant detection allows for the application of the method proposed in the monitoring of the odorant concentration in natural-gas pipelines. An acceptable measurement accuracy is reached at the measurement conditions corresponding to the natural-gas composition. In the mixtures with a dominant (higher than 98%) methane concentration, the measurements can be performed at atmospheric pressure of gases, whereas, in the mixtures with a relatively low methane concentration, gas evacuation to a level of 70–100 torr is needed.

INTRODUCTION

The secure and effective functioning of gas pipelines providing natural gas for both industrial enterprises and dwellings is a topical problem. It is known that natural gas is odorless. Therefore, to prevent accidents and to detect leaks, the gas is odorized to give it a characteristic odor. Mercaptan mixtures are most often used as odorants. Note that the odorant concentration in the gas pipelines should be fixed, since, at low concentrations, operation of the pipelines becomes insecure, but excessive concentrations can be dangerous for the environment. In addition, the problem of odorant excess is important for chemical enterprises, since mercaptan burning yields toxic oxides.

Monitoring of the odorant content in natural gas is discussed in many works (see, for example, [1–5]). In particular, the operation principles of liquid odorizers (setups for the automatic control of a constant odorant concentration in natural gas) are discussed in [1–3]. Marshall and Zeck [4] report on a chemical injection system allowing for the controlled addition of liquid chemical reagents (in particular, odorants) to gases. Verma and Knight [5] have developed a colorimetric method to determine the mercaptan concentration in odorized gas based on the chemical reactions of the odorant with various reagents (e.g., N-ethylmaleimide and alkali hydroxide).

A significant disadvantage of the aforementioned and alternative methods and means of odorant monitoring is their inability to perform highly sensitive detection in real time.

The most promising methods for solving this problem are the methods of optical spectroscopy that employ laser systems and the computer processing of

experimental data. Specifically, our recent experimental results show that a relatively high sensitivity of odorant detection can be reached using absorption spectroscopy in the near-IR spectral range (the wavelength intervals 2.8–4 and 6.5–16 μm) [6, 7].

One of the main difficulties in the practical application of the absorption technique for odorant detection is related to the measurements, in the presence of a background, of the components inherent in an industrial gas mixture (IGM). The absorption spectra of these components can substantially overlap with the odorant absorption spectrum. Note that, at typical IGM pressures in pipelines of 1–12 atm, the odorant consumption is about 16 g per 1000 m^3 (in other words, the concentration of the IGM components is greater than the odorant concentration by a few orders of magnitude). Therefore, the odorant-detection technique must be capable of performing odorant concentration measurements at a level of $1.5 \times 10^{14} \text{ cm}^{-3}$.

The purpose of this work is to develop an absorption technique for real-time odorant detection in gas pipelines at various pressures.

COMPOSITION OF GAS MIXTURES

The main IGM components are methane, ethane, propane, butane, and pentane. Methane is the dominant component, whose concentration varies from 63.7 to 99.2% depending on the gas field [8]. In the mixtures with a relatively low methane content, the concentrations of ethane and pentane can reach 10%. Normally, the total relative concentration of butane and pentane is no greater than 2%. In addition, IGMs may contain such impurities as hydrogen sulphide, carbon dioxide,

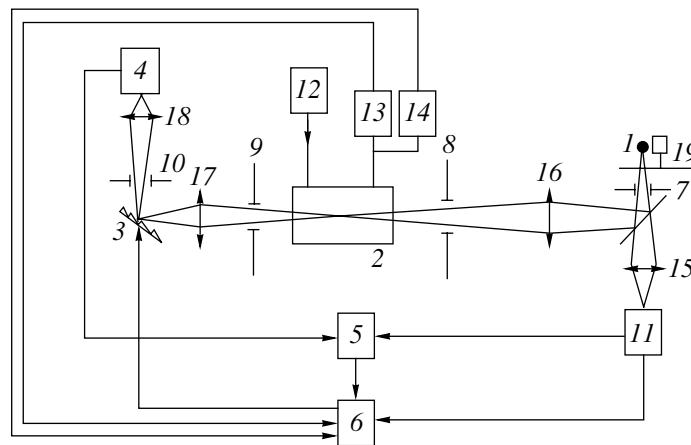


Fig. 1. Scheme of the experimental setup: 1 IR source, 2 absorbing cell, 3 diffraction grating, 4 and 11 IR photodetectors, 5 lock-in detector, 6 computer, 7–10 pinholes, 12 exhaust cart, 13 vacuum gauge, 14 thermometer, 15–18 focusing lenses, and 19 modulator.

and molecular nitrogen, whose total concentration is no greater than 1–1.5%.

In this work, two typical mixtures serve as IGMs. The first mixture contains methane (63.7% vol %), ethane (10.2%), propane (12.6%), pentane (1%), CO₂ (1%), and N₂ (0.6%). The second mixture contains methane (98.8% vol %), ethane (0.07%), pentane (0.01%), CO₂ (0.29%), and N₂ (0.8%).

We choose these mixtures for the following reasons: the first one is characterized by the lowest methane content and the maximum content of ethane and propane, and the second one exhibits the maximum methane concentration.

IGMs are odorized using a variety of odorizing mixtures containing aromatic substances [9]. In Russia, a natural odorizing mixture is used. This mixture consists of organic hydrogen sulphide-containing substance (mercaptans) with the following composition: ethylmercaptan (41.3%), isopropylmercaptan (36.2%), sec-butylmercaptan (10.8%), n-propylmercaptan (6.6%) isobutylmercaptan (2.3%), tert-butylmercaptan (1.43%), and n-butylmercaptan (1.3%) [10]. The unfixed content of mercaptan sulfur and frequent violations of the complex odorant-transporting technique also represent serious obstacles for high-quality gas odorization.

EXPERIMENTS

We experimentally study the IR absorption spectra of the odorant and of an IGM.

Figure 1 shows the scheme of the experimental setup. In the experiments, we employ radiation from an IR source (1) modulated at a frequency of 500 Hz. This radiation is focused in an absorbing cell (2) with a length of 10 cm. The radiation that has passed through the cell is focused on a diffraction grating (3) with a working range of 2.5–25 μm and a spectral resolution of 3 nm. The spectrum is measured with an IR photode-

tector (4), whose signal is fed to the input of a lock-in detector (5) with a bandwidth of 0.03 Hz and, then, to the ADC of a computer (6).

In the experiments, the main sources of noise limiting the sensitivity are the external radiation (stray light) scattered by the windows and inner surfaces of the absorbing cell and the instability of the radiation source. For the rejection of stray light, we employ a series of pinholes (7)–(10) placed on the optical axis. To take into account the light-source instability, we simultaneously detect the radiation intensity behind the cell and in front of it using an IR photodetector (11). Using the aforementioned methods, we diminish the noise to a level of no greater than 0.1%, which is significantly lower than the noise related to the light-source instability.

To be able to perform experiments at various concentrations of the substances under study, we fit the cell to an exhaust cart (12). The gas pressure and temperature in the cell are controlled using a vacuum gauge (13) and a thermometer (14).

Figure 2 demonstrates the absorption spectra of the odorant and the first unodorized IGM in a spectral range of 2.5–17 μm measured at atmospheric pressure. On the vertical axis, we plot the absorption coefficient represented as

$$\alpha(\lambda) = \frac{1}{L} \ln \frac{I_0(\lambda)}{I(\lambda)}, \quad (1)$$

where L is the cell length; I_0 and I are the intensities of radiation that have passed through the cell in the absence and in the presence of the absorbing substance, respectively; and λ is the wavelength of the radiation source.

It is seen that the substances under study exhibit two developed absorption bands, with the maximum absorption corresponding to wavelengths of 3–4 and 6–8 μm. An analysis of the spectra obtained shows that the

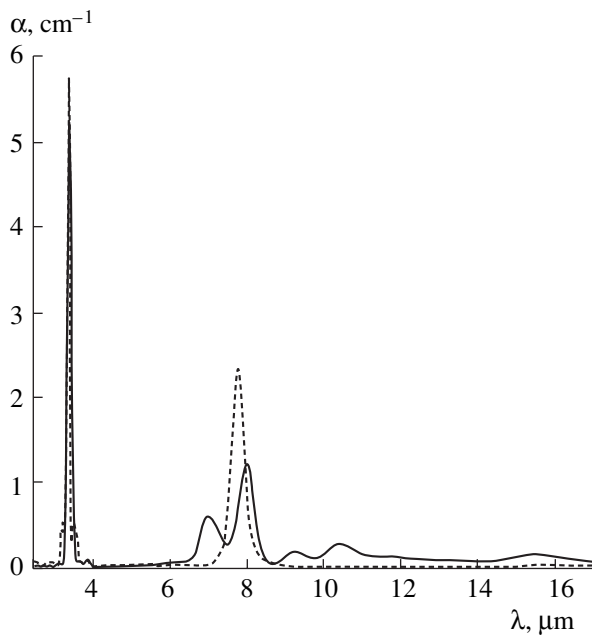


Fig. 2. Absorption spectra of (solid line) odorant and (dashed line) the first IGM.

short-wavelength range cannot be used for odorant detection, since, in this range, the odorant and IGM absorption spectra almost completely overlap. In the second spectral range, we observe a few absorption bands of the odorant that do not coincide with the IGM absorption bands. Therefore, it is expedient to employ this range for estimating the odorant-detection sensitivity and the accuracy of odorant detection in a mixture with the remaining gas components.

Figure 3 shows the absorption coefficients of the odorant and the first IGM in a spectral range of 5–17 μm . It is seen that the odorant exhibits five relatively intense absorption bands centered at 15.75, 10.4, 9.1, 8.06, and 6.94 μm . The IGM exhibits a single strong band with a central wavelength of 7.7 μm and two weak bands with central wavelengths of 12.2 and 6.87 μm . An analysis of the absorption spectra of the first and second mixtures (Fig. 4) shows that the strong band is related to methane absorption, whereas the weak bands are assigned to the ethane and propane present in the first mixture.

METHOD OF MEASURING THE ODORANT CONCENTRATION

The analysis of the results obtained makes it possible to estimate the sensitivity of odorant detection using the absorption technique and to propose a method to determine the odorant concentration in a gas mixture.

For convenience in further analysis, we employ the absorption cross section given by $\sigma(\lambda) = \alpha(\lambda)/n$ (n is the concentration of the substance under study).

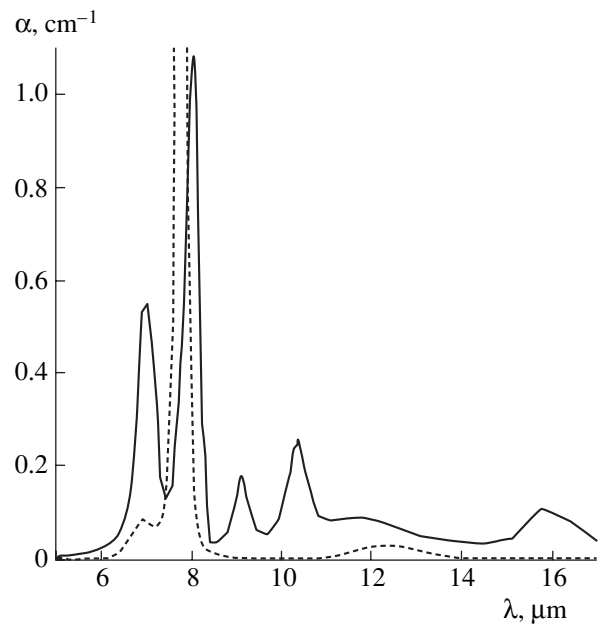


Fig. 3. Absorption coefficients of (solid line) odorant and (dashed line) the first IGM.

To estimate the sensitivity, we use expression (1) to determine the odorant concentration with allowance for the experimental error:

$$n = \frac{1}{\sigma(\lambda)L} \ln\left(\frac{I_0(\lambda)}{I(\lambda)}\right) \pm \frac{10^{-3}}{\sigma(\lambda)L}.$$

The best sensitivity is reached at wavelengths corresponding to the maximum cross sections of the given

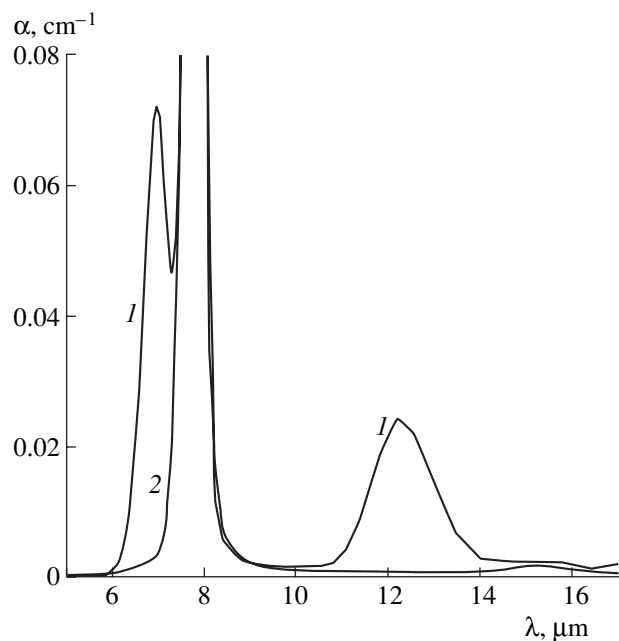


Fig. 4. Absorption spectra of (1) the first and (2) second IGMs.

substance. If the concentration-detection limit is determined from the conventional condition that the signal-to-noise ratio equals unity, then

$$n_{\min} = \frac{10^{-3}}{\sigma_{\max} (8.06 \mu\text{m}) L} \approx 8.9 \times 10^{15} \text{ cm}^{-3}$$

at a cell length of 10 cm.

It is seen from this expression for the detection minimum that the needed sensitivity can be reached if the cell length is increased by a factor of 60, which is quite possible for the multipass cells. In particular, we perform further investigations using a cell with a length of 40 cm and 80–85 passes. The total cell length is 3200–3400 cm. In this case, the minimum detected absorption coefficient is about $3 \times 10^{-7} \text{ cm}^{-1}$, and the odorant concentrations can be detected at a level of $6 \times 10^{13} \text{ cm}^{-3}$.

In spite of the fact that the sensitivity obtained is sufficient for the odorant-concentration measurements, the problem of odorant detection in a gas mixture cannot be solved when the measurements are performed at a single wavelength. To solve this problem, we need to use methods involving simultaneous measurements of the transmitted radiation intensity at several wavelengths. Additional study is needed to specify these wavelengths and to determine their number.

Let $\sigma_o(\lambda_i)$ and $\sigma_g(\lambda_i)$ ($i = 1, \dots, n$) be the odorant and IGM cross sections, respectively, at wavelengths $\lambda_1, \dots, \lambda_n$. Then, under the assumption that the variation in the intensity of radiation that has passed through the cell obeys the Bouguer law

$$I(\lambda) = I_0(\lambda) \exp\{-(n_o \sigma_o + n_g \sigma_g)L\}$$

(where n_o and n_g are the odorant and IGM concentrations, respectively, in the mixture under study), we obtain the following system of equations in terms of n_o and n_g :

$$n_o \sigma_o(\lambda_1) + n_g \sigma_g(\lambda_1) = \frac{1}{L} \ln\left(\frac{I_0(\lambda_1)}{I(\lambda_1)}\right),$$

.....

$$n_o \sigma_o(\lambda_n) + n_g \sigma_g(\lambda_n) = \frac{1}{L} \ln\left(\frac{I_0(\lambda_n)}{I(\lambda_n)}\right).$$

We experimentally measure the intensities of the incident and transmitted radiation. Therefore, we can solve this system if the measurements are performed at two wavelengths. Note the following facts:

(i) If $n = 2$, the solution to the system is written in the following way with allowance for the experimental error of the intensity measurements:

$$\begin{aligned} & (n_o) \\ &= \frac{\sigma_g(\lambda_1) \ln(I_0(\lambda_1)/I(\lambda_1)) - \sigma_g(\lambda_2) \ln(I_0(\lambda_2)/I(\lambda_2))}{(\sigma_o(\lambda_2)\sigma_g(\lambda_1) - \sigma_o(\lambda_1)\sigma_g(\lambda_2))L} \\ & \pm \frac{10^{-3}}{L} \frac{\sqrt{\sigma_g^2(\lambda_1) + \sigma_g^2(\lambda_2)}}{\sigma_o(\lambda_2)\sigma_g(\lambda_1) - \sigma_o(\lambda_1)\sigma_g(\lambda_2)}. \end{aligned}$$

In this case, the minimum detected odorant concentration is given by

$$(n_o)_{\min} = \frac{10^{-3}}{L} \left| \frac{\sqrt{\sigma_g^2(\lambda_1) + \sigma_g^2(\lambda_2)}}{\sigma_o(\lambda_2)\sigma_g(\lambda_1) - \sigma_o(\lambda_1)\sigma_g(\lambda_2)} \right|_{\min}.$$

It is seen that $(n_o)_{\min}$ strongly depends on the wavelengths of measurements.

(ii) Both the radiation intensities and the odorant and IGM cross sections are determined with errors. Hence, we obtain a heterogeneous system of equations $Ax \approx b$:

$$\begin{aligned} A &= \begin{pmatrix} \sigma_o(\lambda_1) & \sigma_g(\lambda_1) \\ \dots & \dots \\ \sigma_o(\lambda_n) & \sigma_g(\lambda_n) \end{pmatrix}, \quad x = \begin{pmatrix} n_o \\ n_g \end{pmatrix}, \\ b &= \frac{1}{L} \begin{pmatrix} \ln\left(\frac{I_0(\lambda_1)}{I(\lambda_1)}\right) \\ \dots \\ \ln\left(\frac{I_0(\lambda_n)}{I(\lambda_n)}\right) \end{pmatrix}. \end{aligned} \tag{2}$$

In general, this system may be either incompatible or indefinite. Hence, the error of the concentrations of the substances under study can be relatively high.

In this case, to increase the accuracy of the solutions, we need to overdetermine the system (i.e., to perform the measurements at more than two wavelengths).

We study system (2) using the least-squares method with the iterative adjustment of roots using the QR expansion of matrix A that results from a series of the orthogonal Householder transforms [11, 12]. A criterion of the accuracy of the solutions obtained is based on the minimization of the following sum of residuals:

$$\min_x \sum_{i=1}^n \sum_{j=1}^2 (b_i - a_{ij}x_j)^2.$$

In the study, we employ the IGM absorption spectra measured at various odorant contents $\delta = n_o/n_g$ ranging from 1000 to 6×10^{-6} (the last value corresponds to a minimum odorant consumption of 16 g/1000 m³). Fig-

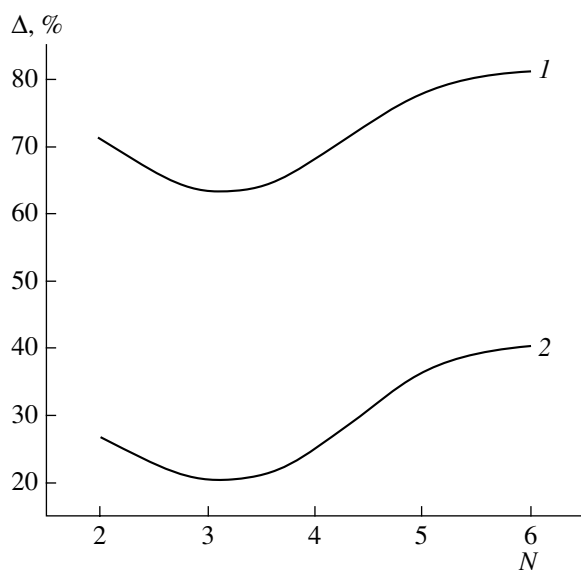


Fig. 5. Plots of the odorant-detection error vs. the number of the measurement wavelengths for (1) the first and (2) second IGMs at $\delta = 6 \times 10^{-6}$.

ure 5 demonstrates the dependence of the relative (with respect to the odorant concentration in the medium) odorant-detection error obtained using the least-squares method at the minimum content ($\delta = 6 \times 10^{-6}$) in the gas mixture on the number of wavelengths used in the measurements. Table shows the wavelengths corresponding to the minimum error. It is seen from Fig. 5 and the table that there exist a few wavelengths corresponding to nearly equal measurement errors. The best accuracy of odorant detection is reached when the measurements are performed at three wavelengths. Two of

them correspond to the odorant absorption maxima most distant from the IGM absorption maximum, and the third wavelength corresponds to the IGM absorption maximum.

A comparison of the results obtained for the first and second IGMs shows that (i) the optimum wavelengths coincide and (ii) the accuracy of odorant detection in the second IGM is 3–3.5 times better than the detection accuracy in the first IGM, which is related to the higher content of ethane and propane in the first mixture (the accuracy is lower owing to the absorption of these gases in the vicinity of the odorant absorption band).

Thus, the results obtained show that the accuracy of odorant detection in IGMs predominantly consisting of methane (whose methane concentration is higher than 95%) is sufficient for the measurements under real conditions. Note that, for IGMs with a relatively low concentration of methane, the error in odorant detection is greater than 60% for the minimum odorant concentration. Hence, in this case, an additional increase in the accuracy is needed.

One of the methods of increasing the accuracy employs an analysis of the effect of the gas-mixture pressure in the absorbing cell on the accuracy and sensitivity of measurements. On the one hand, a decrease in the pressure leads to a decrease in the odorant absorption coefficient, which is related to a decrease in its total concentration. This results in a worsening of the sensitivity. On the other hand, in the IR spectral range, the broadening of the absorption bands of the substances under study is predominantly determined by the collisions, and the bands have Lorentzian shapes. A decrease in the pressure causes a decrease in absorption at the Lorentz wings and an increase in absorption at the central wavelengths. This means that the measured absorption cross sections of the odorant and IGM

Table

$\lambda_1, \mu\text{m}$	$\lambda_2, \mu\text{m}$	$\lambda_3, \mu\text{m}$	$\lambda_4, \mu\text{m}$	$\Delta, \%$							
				$\delta = 10^{-3}$		$\delta = 10^{-4}$		$\delta = 10^{-5}$		$\delta = 6 \times 10^{-6}$	
				IGM (I)	IGM (II)	IGM (I)	IGM (II)	IGM (I)	IGM (II)	IGM (I)	IGM (II)
15.75	7.7	–	–	0.38	0.12	3.63	1.3	36.4	12.4	82.8	26.4
10.4	7.7	–	–	0.32	0.09	2.9	0.9	29.5	9.6	70.9	22.3
9.1	7.7	–	–	0.44	0.14	4.36	1.6	43.2	14.2	91.3	28.4
10.4	8.06	–	–	0.46	0.12	4.18	1.5	40.3	13.8	88.7	27.2
10.4	8.06	–	–	0.41	0.16	3.6	1.35	36.4	11.4	82.8	26.5
15.75	10.4	7.7	–	0.27	0.08	2.86	0.85	28.8	9.5	60.3	20.5
15.75	9.1	7.7	–	0.35	0.11	3.6	1.2	36.3	11.8	83.7	26.8
15.75	10.4	8.06	–	0.43	0.13	4.44	1.45	40.1	12.5	88.5	27.1
15.75	10.4	6.94	–	0.38	0.12	3.58	1.4	35.7	12.1	82.1	26.2
15.75	10.4	9.1	7.7	0.29	0.11	2.92	0.95	29.5	8.9	67.1	25.3
15.75	10.4	9.1	6.94	0.4	0.12	3.8	1.4	38.1	12.2	87.6	26.8

may significantly depend on the pressure. Therefore, when the gas under study is evacuated from the absorbing cell at a constant pressure ratio $\varepsilon = p_o/p_g$ of the odorant and IGM, a possible variation in the ratio of the absorption coefficients is determined by a variation in the ratio of the cross sections:

$$\frac{\alpha_o(p)}{\alpha_g(p)} = \frac{\sigma_o(p)}{\sigma_g(p)} \varepsilon.$$

Therefore, if the odorant is detected at one of the wavelengths corresponding to the odorant absorption maximum, the ratio of the absorption coefficients may increase with decreasing pressure. This will lead to a decrease in the relative contribution of IGM to the detected variation in the transmitted intensity.

Note also that, when the odorant and IGM absorption coefficients depend on the pressure, the corresponding dependences of the variation in the intensity of radiation that has passed through the cell can be nonlinear. This nonlinearity leads to a worsening of the measurement accuracy. Therefore, we need to determine the cross sections of the substances under study at various pressures.

Figure 6a shows the dependence of the odorant absorption cross section at the central wavelengths of the absorption bands on the odorant concentration (the measurements are performed at a fixed temperature and various pressures of the gas mixture in the cell). It is seen that, in the entire range of pressures (up to atmospheric pressure), the odorant absorption cross section remains virtually constant within experimental error. A possible reason for this lies in the fact that the absorption of the polyatomic odorant molecules is determined by a large number of overlapping bands, whose broadening does not affect the integral absorption cross section. Figure 6b shows a similar dependence obtained for the unodorized first IGM at the same wavelengths lying far from the center of its absorption maximum. It is seen that an increase in the pressure leads to an increase in the absorption cross section, which is related to an increase in the absorption at the wings of the Lorentz band.

The measurements of the absorption cross sections of the unodorized first and second IGMs at the central wavelengths of the absorption bands of their components show that, as in the case of the odorant, the cross sections are virtually independent of the pressure.

Thus, the contributions of the odorant and IGM to the absorption are different at different pressures. Hence, it is expedient to perform studies aimed at optimizing the pressure of the gas mixture under consideration with respect to the sensitivity and accuracy of measurements.

Figure 7 shows the dependence of the odorant detection error on the pressure in the cell (ranging from 10 torr to atmospheric pressure) at various odorant concentrations in the gas mixture. The dependence is obtained for measurements at the three wavelengths

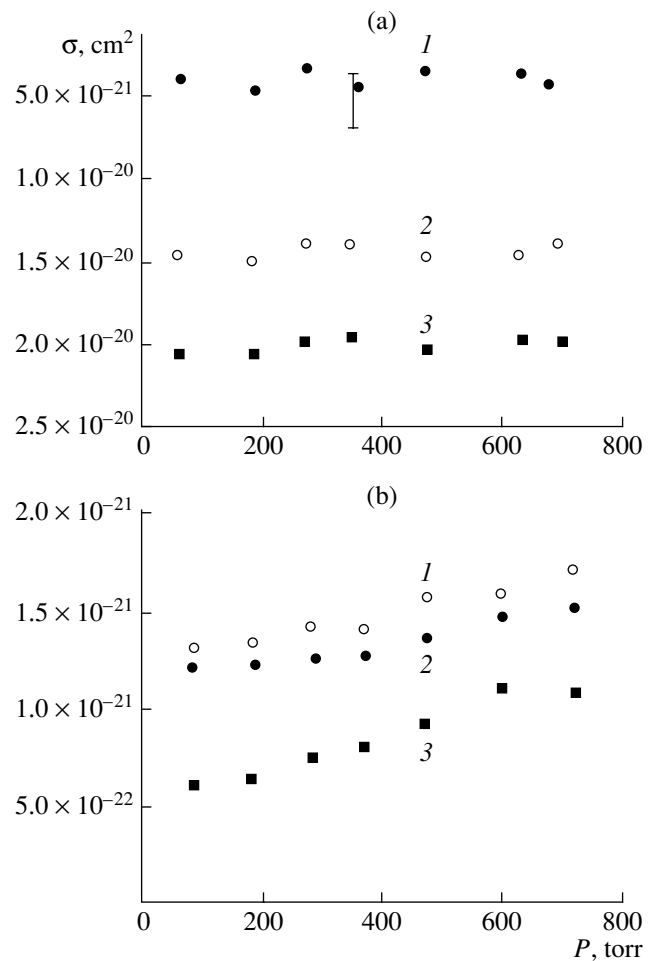


Fig. 6. Plots of (a) the odorant and (b) the first IGM absorption cross sections vs. pressure at wavelengths of (1) 8.06, (2) 6.94, and (3) 10.4 μm .

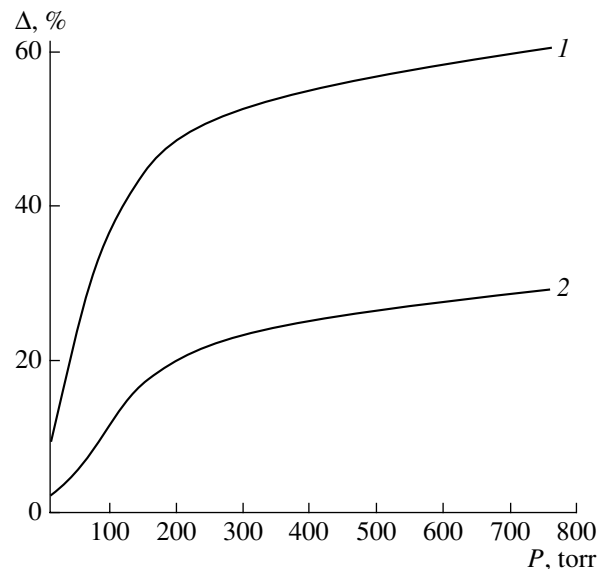


Fig. 7. Plots of the odorant-detection error vs. the pressure of the first IGM for $\delta = (1) 6 \times 10^{-6}$ and (2) 10^{-5} .

corresponding to the minimum error of measurements at atmospheric pressure. It is seen that the measurement error significantly depends on the pressure of the mixture under study. In particular, for a relative odorant content of $\delta = 6 \times 10^{-6}$, an increase in the pressure from the atmospheric level to 10 torr results in a decrease in the odorant detection error to 10%. This corresponds to sixfold increase in the measurement accuracy in comparison to the measurements performed at atmospheric pressure. In our opinion, the acceptable measurement accuracy corresponds to an error of 20–30% (this error is realized upon the odorant detection in the second IGM at atmospheric pressure) that is reached when the pressure of the gas mixture decreases to 70–100 torr.

Note that a decrease in the pressure leads to a worsening of the measurement sensitivity owing to a decrease in the absorption coefficient. Therefore, the measurements at a relatively low pressure must be performed using an absorption cell with a proportionally increased length. This can be realized when the number of passes increases in the multipass cells.

CONCLUSIONS

The results obtained show that the absorption method can be used to detect odorants of natural gas in gas pipelines in real time. An acceptable measurement accuracy is reached under measurement conditions depending on the composition of the natural gas. In the mixtures with a relatively high (greater than 98%) methane concentration, the measurements can be performed at atmospheric gas pressure. In the mixtures

with a relatively low methane concentration, the gas pressure must be decreased to a level of 70–100 torr.

REFERENCES

1. A. D. Agarkov, V. I. Nikishin, A. V. Novikov, *et al.*, RF Patent No. 2 056 919 (1994).
2. E. Smars, US Patent No. 5632295 (1997).
3. E. Smars, RF Patent No. 2083641 (1997).
4. S. E. Marshall and M. V. Zeck, US Patent No. 6208913 (2001).
5. A. Verma and A. R. Knight, US Patent No. 3960494 (1976).
6. S. V. Kireev, E. M. Podolyako, and S. L. Shnyrev, in *Abstracts of Scientific Session of MEPHI-2003* (2003), Vol. 4, p. 19.
7. S. V. Kireev, E. M. Podolyako, N. G. Petrov, and S. L. Shnyrev, in *Abstracts of 6th International Scientific Conference on Molecular Biology, Chemistry, and Physics of Heterogeneous Systems* (Moscow–Ples, 2004), pp. 249–251.
8. A. V. Gromov, N. E. Guzanov, and A. Hachikyan, *Handbook on Exploitation of Gas Pipelines* (Nedra, Moscow, 1987), p. 176 [in Russian].
9. A. N. Yanovich and I. Borshenko, *Safety Engineering of Gas Pipelines* (Nedra, Moscow, 1984), p. 256 [in Russian].
10. N. I. Podlegaev, Technical Conditions TU 51-31323949-94-2002 (OOO Vniigaz, Moscow, 2002).
11. A. George and J. W. H. Liu, *Computer Solution of Large Sparse Positive-Definite Systems* (Prentice-Hall, Englewood Cliffs, N.J., 1981; Mir, Moscow, 1984).
12. R. J. Hanson, *SIAM J. Sci. Comput. (USA)* **7**, 3 (1986).